

Approximate solutions for developing shear dispersion with exchange between phases

By C. G. PHILLIPS AND S. R. KAYE

Physiological Flow Studies Group, Centre for Biological and Medical Systems,
Imperial College of Science, Technology and Medicine, Prince Consort Road,
London SW7 2BY, UK

(Received 22 October 1997 and in revised form 8 May 1998)

We consider the transport of a tracer substance in Poiseuille flow through a pipe lined with a thin, fixed wall layer in which the tracer is soluble. A formal solution is given for the variation of concentration with time at a fixed downstream position following an initial release of tracer. Asymptotic approximations are derived assuming that: (i) the Péclet number is large; (ii) the time scale for diffusion across the wall layer is much larger than that for diffusion across the fluid phase and (iii) the dimensionless distance downstream of the point of release, z , is large. This means that the transverse concentration variation is small within the fluid phase, so that transport is dominated by the exchange of tracer between the phases and radial diffusion within the wall layer. The character of the concentration transient is found to be determined by two dimensionless numbers, an absorption parameter κ and an effective wall layer thickness ν (both rescaled to take account of the ratio of diffusivities in the two phases); by assumption (ii), ν is large. Several different regimes are possible, according to the values of κ , ν and z . At sufficiently large distances, a Gaussian approximation, analogous to Taylor's solution, is applicable. At intermediate distances, provided κ is not too large, a highly skewed transient is predicted. If κ is small, there exists another region further upstream where the effect of the wall is negligible, and Taylor's Gaussian approximation applies. More complicated behaviour occurs in the zones of transition between these three regions. The behaviour described is expected to be typical of a range of similar systems. In particular, it may be shown that the basic form of the skewed approximation is insensitive to the geometry of the system, and also applies when the Péclet number is of order unity.

1. Introduction

In this paper we consider the transport of a tracer substance in a two-phase system consisting of a flowing phase, where both advection and diffusion occur, and a fixed phase, in which the tracer moves by diffusion alone. Systems of this general type are of common occurrence, and their study has been motivated by a wide range of applications. For example, in chemical engineering, theoretical descriptions have been sought for the process of gas chromatography in coated tubes and other systems (e.g. Westhaver 1942; Golay 1958). Biological applications have also been prominent, and include gas transport in the microcirculation (e.g. Lenhoff & Lightfoot 1984) and the conducting airways (e.g. Davidson & Schroter 1983). More generally, such systems have been treated as models for the effects of regions of slow flow on shear dispersion, such as the viscous sub-layer in turbulent flow (e.g. Chatwin 1973) and 'dead zones' in rivers (e.g. Purnama 1988).

Transport in such systems, containing both a flowing and a fixed phase, is essentially analogous to the shear dispersion process considered by Taylor (1953), in which, sufficiently long after the release of a tracer substance, the combined effect of diffusive radial movement and the radial variation of velocity in Poiseuille flow is equivalent to an enhancement of axial diffusion. As a result, the concentration distribution may eventually be described approximately by a Gaussian function of axial distance. The rate of change of the mean of this Gaussian is equal to the average fluid velocity, and half of the rate of change of its variance gives the effective axial diffusivity, or dispersion coefficient. In a system containing two phases, the diffusive movement of the tracer, not only within the fluid but also between the phases, results in a similar enhancement of axial diffusivity, which is potentially even greater than that in a single phase. In fact, this effect was studied theoretically in a two-phase system (Poiseuille flow through a pipe lined with a thin, highly absorbent layer) by Westhaver (1942), who calculated the dispersion coefficient for this case a decade before Taylor's work. (In a related problem, the same author also anticipated (in 1947) Taylor's calculation of the dispersion coefficient for Poiseuille flow in the absence of a wall layer.) Golay (1958) and Aris (1959) later generalized Westhaver's result to a wider class of tubular systems. Since then, the problem of determining the dispersion coefficient has been formulated for a very general class of periodic porous media, including those in which diffusion within the fixed phase is important (Brenner & Adler 1982).

In the two-phase system, just as in Taylor's problem, the concentration distribution becomes approximately Gaussian at sufficiently large times. This is true whether we consider the axial distribution of concentration at a fixed time, or its temporal variation at a fixed position. However, dispersion becomes fully developed only after there has been time for tracer to diffuse over the whole cross-section of the system. In Taylor dispersion, the tracer distribution at times earlier than this is known to be markedly non-Gaussian (see e.g. Phillips & Kaye 1996, 1997), and this may be important for transport through short tubes, or at very high flow rates. Similarly, in the two-phase system the Gaussian concentration distribution does not become fully developed until tracer has had time to diffuse across the fixed, as well as the fluid phase. In the present work, where diffusion across the fixed phase is assumed to take much longer than that across the fluid, the non-Gaussian stage in the development of shear dispersion may persist for a significant time.

The most popular technique which has been used to study dispersion in two-phase systems is a natural extension of the formulations of Golay (1958) and Aris (1959), who calculated the fully developed dispersion coefficient by considering the rate of change of the axial variance of the tracer distribution. Accordingly, several workers have characterized the development of dispersion, and the influence of exchange between phases, in terms of the axial moments of the tracer distribution as functions of time. For example, Chatwin (1973) considered the axial variance and its time-derivatives for a two-phase system intended to model the effect of the viscous sub-layer on dispersion. Reis *et al.* (1979) considered dispersive transport through a column packed with permeable spheres, using the method of Gill & Sankarasubramanian (1970), in which an effective transport equation is formulated in terms of a sequence of time-varying effective transport coefficients, related to the rates of change of the axial moments. Higher-order moments at large times (as far as the kurtosis of the concentration distribution) were calculated by Purnama (1988), for a general model of the influence of dead zones on dispersion in streams. Davidson & Schroter (1983) calculated numerically effective transport coefficients defined in terms of the time-derivatives of the axial mean and variance of concentration in the fluid, for the same

two-phase system considered in the present work, namely Poiseuille flow through a pipe lined with a wall layer, within which the tracer may diffuse. A more analytic approach to the same problem was later adopted by Phillips, Kaye & Robinson (1995). However, as they pointed out, in the long period before dispersion is fully developed, when the concentration distribution is far from being Gaussian, the moments give little information about the actual form of the concentration profile. Instead, they reflect the character of the long, gradually decaying tail of the distribution, which results from the delay of tracer transport by absorption in the wall layer.

An alternative to the calculation of moments, popular in the chemical engineering literature, is to consider a simpler, one-dimensional model problem, in which average concentrations and effective velocity and dispersion coefficients are assigned to each phase separately, and the rate of exchange between phases is assumed to depend linearly on the local average concentrations. This simplification allows further analytic progress to be made in investigating the role of exchange in modifying dispersive transport (see e.g. Lenhoff & Lightfoot 1984). Such an approach may be particularly useful if resistance to exchange between the phases is more important than diffusive resistance within the phases. Similarly, the formulation of Balakotaiah & Chang (1995), which resolves the transverse concentration distribution within the fluid, but employs an averaged concentration in the wall layer, is appropriate if diffusive resistance within the fluid is the limiting factor. However, for the system considered in the present work, diffusive resistance within the wall layer is high, and the consequent radial non-uniformity of concentration plays a dominant role.

More closely related to the present work is the study of Young (1988), who formulated a model problem in which the tracer concentration within a pipe is described by an one-dimensional, averaged equation, and there is diffusive exchange with stagnant side branches, within which the concentration distribution is non-uniform. Young calculated exactly the axial moments of the tracer distribution as functions of time, laying stress on their 'non-diffusive' growth at times before the full development of shear dispersion. When, in Young's notation, $\Delta \ll 1$, his model becomes mathematically equivalent to the present one at sufficiently large distances (namely in the intermediate region treated in §3.1, and further downstream), with the stagnant side-branches fulfilling the same role as our wall layer. In this regime, there is a balance between axial convection in the pipe and transverse diffusion in the wall layer (or side branches). Although Young did not calculate the concentration distribution within the pipe, he gave an approximate solution for the concentration within the side branches (his equation (3.17)). At leading order, in the main part of the temporal range, this solution represents a radially integrated version of the expression (3.2) for tracer concentration in the wall layer, derived below. (The temporal range of validity of Young's solution is slightly more limited than that of (3.2), because in deriving it he neglected an additional term of the governing equation, which requires $t \gg \kappa z^{3/2}$ in our notation.)

Finally, for the system considered in this paper, concentration transients have been found by direct numerical calculation (Shankar & Lenhoff 1991). However, in contrast to the present work, these calculations treat cases in which the time required for diffusion across the wall layer is comparable with, or smaller than, that for diffusion across the fluid phase, so comparison with the present results is not possible.

In contrast to previous work, particularly methods based on the calculation of spatial moments, our approach in this paper is to derive asymptotic approximations for the tracer concentration distribution, and to work in terms of the temporal variation of concentration at a fixed position, rather than the axial variation at

a fixed time. The method, in which approximations for the Laplace transform of the concentration field are employed, is closely related to that used in our previous investigations of the development of Taylor dispersion (Phillips & Kaye 1996, 1997). To simplify the mathematical details, we assume that the Péclet number, expressing the importance of advection relative to (axial) diffusion, is very large, and that the wall layer is sufficiently thin that its curvature may be ignored. Furthermore, we assume that the diffusivity within the wall layer is much smaller than that in the fluid phase, and that as a result the time scale for diffusion across the wall layer is much larger than that across the fluid. We restrict our attention to distances sufficiently large that the radial tracer distribution within the fluid is nearly uniform during the main part of the concentration transient.

In summary, the outline of the paper is as follows. In §2 the problem is formulated mathematically, an exact formal solution is given, and the general procedure for obtaining approximations is outlined. In §3, we derive approximations for the concentration transient applicable in three different regions, as determined by the downstream distance of the point of observation from the point where tracer is released: a skewed approximation valid at intermediate distances, and Gaussian distributions appropriate further upstream and downstream. We also give transitional forms appropriate near the boundaries between these regions. The relationship of these approximations is illustrated by numerical results in §4, and their applicability is discussed in §5.

2. Mathematical formulation

2.1. Formal solution

We consider transport of a tracer substance through a system consisting of a circular pipe of radius a surrounded by an annular wall layer of thickness h . The pipe contains flowing fluid, through which tracer is transported by both advection and diffusion, but the wall layer is stationary, so that only diffusion acts within it. The tracer is assumed to be introduced instantaneously at some point within the fluid, and the Green's function solution for the subsequent concentration distribution is sought. Throughout this paper, the fluid will be assumed to move with a fully developed (parabolic) Poiseuille flow profile. If tracer concentration is denoted by C , time by T , axial distance by Z , transverse position by \mathbf{R} , the axial velocity by $V(\mathbf{R})$ and the diffusivities by D and D_w in the fluid and the wall layer respectively, the governing equations are

$$\left. \begin{aligned} \frac{\partial C}{\partial T} + V(\mathbf{R}) \frac{\partial C}{\partial Z} &= D \left(\nabla_{\mathbf{R}}^2 C + \frac{\partial^2 C}{\partial Z^2} \right) & \text{for } R < a, \\ \frac{\partial C}{\partial T} &= D_w \left(\nabla_{\mathbf{R}}^2 C + \frac{\partial^2 C}{\partial Z^2} \right) & \text{for } a < R < a + h, \end{aligned} \right\} \quad (2.1)$$

in which $\nabla_{\mathbf{R}}$ represents the transverse component of the differential operator ∇ .

The boundary conditions at the interface between the two phases are

$$\lambda \frac{\partial C}{\partial R} \Big|_{R=a^+} = \frac{\partial C}{\partial R} \Big|_{R=a^-}, \quad C|_{R=a^+} = \beta C|_{R=a^-}; \quad (2.2)$$

in the first, which represents the continuity of normal flux, λ is defined as the ratio of diffusivities in the wall layer and fluid, D_w/D ; in the second, it is assumed that the ratio of the tracer concentrations immediately adjacent to the interface is equal to β ,

its equilibrium value (that is, there is no local resistance to exchange of the tracer across the interface). It is also assumed that the outer boundary of the wall layer is impermeable to the tracer, so that

$$\left. \frac{\partial C}{\partial R} \right|_{R=a+h} = 0. \quad (2.3)$$

(The general solution presented in this subsection would be equally applicable for the alternative condition $C = 0$ at $R = a + h$, representing perfect absorption at the outer boundary, or indeed, for any linear, homogeneous condition on C and $\partial C/\partial R$; cf. Phillips *et al.* 1995.)

In order to express the problem in dimensionless form, we denote by V_m the average value of the axial velocity over the cross-section. Then the strength of advection relative to axial diffusion is expressed by the Péclet number

$$P = V_m a / D. \quad (2.4)$$

Dimensionless variables are defined by

$$c = \pi \mathcal{M}^{-1} P a^3 C, \quad \mathbf{r} = a^{-1} \mathbf{R}, \quad z = P^{-1} a^{-1} Z, \quad t = a^{-2} D T. \quad (2.5)$$

The definition of c , in which \mathcal{M} denotes the total mass of tracer present in the system, results in a convenient normalization of the dimensionless problem. The resulting dimensionless governing equation is

$$\left. \begin{aligned} \frac{\partial c}{\partial t} + v(\mathbf{r}) \frac{\partial c}{\partial z} &= \nabla_{\mathbf{r}}^2 c + P^{-2} \frac{\partial^2 c}{\partial z^2} & \text{for } r < 1, \\ \frac{\partial c}{\partial t} &= \lambda \left(\nabla_{\mathbf{r}}^2 c + P^{-2} \frac{\partial^2 c}{\partial z^2} \right) & \text{for } 1 < r < 1 + \epsilon, \end{aligned} \right\} \quad (2.6)$$

in which $v(\mathbf{r}) = V(\mathbf{R})/V_m = 2(1 - r^2)$ is the dimensionless axial fluid velocity, and $\epsilon = h/a$ is the dimensionless wall layer thickness. The conditions on c at the interface and at the outer boundary of the wall layer are identical in form to (2.2), (2.3).

Since the problem is linear, the solution corresponding to an arbitrary initial distribution of tracer within the fluid phase may be expressed in terms of a Green's function $G(\mathbf{r}, z, t; \mathbf{r}_0)$, satisfying the initial condition

$$G(\mathbf{r}, z, 0; \mathbf{r}_0) = \pi \delta(\mathbf{r} - \mathbf{r}_0) \delta(z), \quad (2.7)$$

in which δ is the Dirac delta function, so that the tracer is assumed to be concentrated at the transverse position \mathbf{r}_0 and at $z = 0$ (without loss of generality); the normalisation is the same as in our earlier treatment (Phillips & Kaye 1996).

The formulation above includes the effects of axial molecular diffusion, and is therefore valid for arbitrary values of the Péclet number P . If the diffusivity were the same in the wall layer and the fluid, it would be possible to express the finite- P solution for c in terms of the corresponding solution in the absence of axial molecular diffusion (that is, the infinite- P solution), simply by convolving the latter with a Gaussian function of z (see, e.g., Phillips & Kaye 1996). But because the diffusivity differs between the two phases, this is not the case here. In principle it would be straightforward to retain the effects of finite P in a derivation similar to that below, at the cost of increased algebraic complexity. However, for the sake of simplicity, in the remainder of this paper we confine ourselves to the limit $P \rightarrow \infty$, so that the terms representing axial diffusivity in (2.6) may be omitted. (In Appendix

B, §B.1, it is demonstrated that one of the approximations derived below, (3.1), is insensitive to this assumption.)

A formal solution to the problem may be obtained by steps exactly similar to those leading to (4.2) of Phillips & Kaye (1996). In summary, a Fourier transform (variable k) with respect to z and a Laplace transform (variable s) with respect to t are applied. The transformed solution has poles in the k -plane, and its behaviour in their neighbourhood is related to an eigenvalue problem (given below). By using Green's theorem, the residues at these poles may be expressed in terms of integrals of the eigenfunctions, allowing the inversion of the Fourier transform, which gives

$$G(\mathbf{r}, z, t; \mathbf{r}_0) = \frac{1}{2\pi i} \sum_{n=0}^{\infty} \int_{\mathcal{C}_n} F_n(\mathbf{r}_0, \mathbf{r}; s) \exp(st - \ell_n(s)z) ds, \quad (2.8)$$

in which

$$F_n(\mathbf{r}_0, \mathbf{r}; s) = \frac{\pi f_n(\mathbf{r}_0; s) f_n(\mathbf{r}; s)}{\int_{r' \leq 1} v(\mathbf{r}') f_n(\mathbf{r}'; s)^2 dA'}, \quad (2.9)$$

where the \mathcal{C}_n are suitably chosen contours of integration, \mathbf{r}' is a dummy integration variable and dA' the corresponding area differential, and the eigenvalues $\ell_n(s)$ and eigenfunctions $f_n(\mathbf{r}; s)$ satisfy the equations

$$\nabla_r^2 f_n = (s - 2\ell_n(1 - r^2)) f_n \quad \text{for } r < 1, \quad (2.10a)$$

$$\nabla_r^2 f_n = \lambda^{-1} s f_n \quad \text{for } 1 < r < 1 + \epsilon, \quad (2.10b)$$

again subject to conditions at $r = 1$ and $r = 1 + \epsilon$ identical in form to (2.2), (2.3). Without loss of generality, we may fix the normalization of the eigenfunctions by specifying $f_n = 1$ at $r = 0$.

In principle, the equations just given constitute an exact solution for the Green's function G . In general, its evaluation would require the eigenfunctions f_n , and the integrals in (2.8) and (2.9), to be computed numerically. However, simpler approximations for the concentration distribution, valid for specified ranges of the governing parameters, may be derived by finding suitable asymptotic approximations for the eigenfunctions and eigenvalues. We have previously considered the case where the wall layer is absent (i.e. the development of Taylor dispersion), and have applied such a strategy to derive two approximations for G : the first valid when the downstream distance z is large (Phillips & Kaye 1996), and the second in the very early stages of the transient (Phillips & Kaye 1997). In the present work, we derive large- z approximations corresponding to the former of these. As in our previous studies, the emphasis will be on the temporal variation of concentration which would be observed at a fixed axial position.

2.2. Simplifying assumptions

In order to simplify the problem, we assume that $\epsilon = h/a$ is small, so that the wall layer is thin relative to the radius of the pipe, and its curvature may be ignored. (Like the assumption that P is very large, discussed above, this simplifies the manipulations involved, but does not change the structure of the solution. In Appendix B it is demonstrated that the approximation (3.1) derived below remains valid for larger values of ϵ .) The governing equation (2.10b) for f_n in the wall layer, subject to an outer boundary condition of the form (2.3), may be solved explicitly and, with the

assumption that ϵ is small, the solution takes the form

$$f_n(r; s) = A_n(s) \cosh(\lambda^{-1/2} s^{1/2} (1 + \epsilon - r)) \quad \text{for } 1 < r < 1 + \epsilon, \quad (2.11)$$

for some function $A_n(s)$. (Note that the condition that the solution f_n decays, rather than grows, with distance into the wall layer requires that $\text{Re } s^{1/2} > 0$, so that, in the definition of $s^{1/2}$, the branch cut must lie along the negative real axis.) The function $A_n(s)$ may be eliminated by combining this solution for f_n in the wall layer with the dimensionless form of the conditions (2.2) at the interface. Thus we obtain the condition at the boundary of the fluid phase:

$$\frac{\partial f_n}{\partial r} = -\kappa' s^{1/2} f_n \quad \text{at } r = 1^-, \quad \text{where } \kappa' = \kappa \tanh(\nu s^{1/2}), \quad (2.12)$$

in which the absorption parameter κ and the effective wall layer thickness ν are the two dimensionless groups through which the parameters β , ϵ and λ influence the solution, defined by

$$\kappa = \beta \lambda^{1/2}, \quad \nu = \epsilon \lambda^{-1/2}. \quad (2.13)$$

These parameters represent versions of the partition coefficient β and wall layer thickness ϵ respectively, rescaled to take account of the difference between the diffusivities in the two phases.

The second simplifying assumption is that the second of these parameters, ν , is large. This implies that the time scale for diffusion across the wall layer is much larger than that for diffusion across the fluid phase. As a result, there are two distinct stages in the development of dispersion: in the first, for smaller distances, the radial concentration distribution within the fluid is non-uniform but tracer penetration into the wall layer is very small; in the second, for larger distances, diffusion within the wall layer in general has a dominant effect, but the radial tracer distribution within the fluid is nearly uniform. (Note that this simplification, unlike the assumptions that P is large and ϵ is small, is essential in making analytic progress possible. If ν were of order unity, it would be necessary to solve the eigenvalue problem numerically in order to obtain non-trivial approximations.)

We seek approximate expressions for the Green's function G , appropriate when z is large, corresponding to the second stage of the development of dispersion, just discussed. Our previous solution for Taylor dispersion suggests that in this regime the leading ($n = 0$) term of the series in (2.8) will be dominant, and may be evaluated approximately by solving the eigenvalue problem (2.10a), (2.12) for f_0 and ℓ_0 , for small values of s . To obtain such a solution, assume initially that s lies within the range $\nu^{-2} \lesssim s \ll 1$. This implies that $\nu s^{1/2}$ is comparable with unity or larger, so that the hyperbolic tangent in (2.12), and therefore the coefficient κ' , may be treated as fixed. The resulting solution is of the form

$$f_0(r; s) = 1 + O(s^{1/2}), \quad \ell_0(s) = m_1 s^{1/2} + m_2 s + m_3 s^{3/2} + m_4 s^2 + O(s^{5/2}), \quad (2.14)$$

in which the coefficients m_j depend on s only through κ' . By straightforward substitution of these series into (2.10a) and (2.12), the first four coefficients are found to be

$$\begin{aligned} m_1 &= 2\kappa', & m_2 &= 1 - \frac{11}{12}\kappa'^2, & m_3 &= -\frac{1}{4}\kappa' + \frac{251}{720}\kappa'^3, \\ m_4 &= -\frac{1}{48} + \frac{11}{96}\kappa'^2 - \frac{5603}{53760}\kappa'^4. \end{aligned} \quad (2.15)$$

Note that this series solution remains valid even if κ' is large, provided that $\kappa' s^{1/2} \ll 1$. In this approximation, f_0 is approximately uniform within the fluid phase. The

physical implications of this are clear by inspection of (2.8), (2.9): at the leading order, during the main part of the transient, the measured concentration is radially uniform in the fluid phase (though not in the wall layer), and is also independent of the transverse position in the fluid where the tracer is released. As discussed below, at sufficiently large distances, dispersion becomes fully developed, and the concentration distribution becomes nearly uniform, even within the wall layer, during the main part of the transient. Mathematically, this regime corresponds to values of s much smaller than v^{-2} . In this case an alternative series solution is obtained by expanding $\tanh(vs^{1/2})$ in powers of $s^{1/2}$ (see §3.3). (Note that, however large the downstream distance, at very early and at very late times the solution for the main part of the transient, corresponding to small values of s , breaks down, and the concentration distribution becomes radially non-uniform. With the assumption that $z \gg 1$, however, the tracer concentration is extremely small whenever this occurs.)

Provided that the integrals in (2.8), (2.9) are dominated by contributions from values of s satisfying both $s \ll 1$ and $\kappa's^{1/2} \ll 1$, we see from (2.14) that f_0 is approximately uniform within the fluid phase, so that the function F_0 defined by (2.9) may be replaced by unity. Thus we obtain

$$G(\mathbf{r}, z, t; \mathbf{r}_0) \sim \frac{1}{2\pi i} \int_{\mathcal{C}_0} \exp(st - \ell_0(s)z) ds. \quad (2.16)$$

The omitted contributions from higher ($n \geq 1$) modes are expected to be exponentially smaller in z than the leading term; the coefficient multiplying z in the exponent depends both on the parameters κ and v , and on the value of t (cf. the discussion of the $\kappa = 0$ case in Phillips & Kaye 1996, Appendix B). The errors arising from the $f_0 \sim 1$ approximation in the leading term are algebraically small in z .

It will be convenient in the remainder of the paper to define a new time variable, namely

$$\Delta t = t - z, \quad (2.17)$$

that is, the time elapsed since z , which is the average time taken for the flowing fluid to reach the observer from the point where tracer is introduced. From (2.14), the exponent in (2.16) is given by

$$st - \ell_0(s)z = s\Delta t - 2\kappa'zs^{1/2} + \frac{11}{12}\kappa'^2zs + \frac{1}{48}zs^2 + O(zs^3, \kappa'zs^{3/2}, \kappa'^3zs^{3/2}) \quad (2.18)$$

when $s, \kappa's^{1/2} \ll 1$. The character of the solution is determined by which of the terms in this equation are significant, and this in turn depends upon the sizes of κ , z and Δt , relative to one another and to v .

In considering the main part of the concentration transient at intermediate distances, it will be useful to employ a rescaled version of s , defined by $\sigma = \kappa^2z^2s$. When σ is of order unity, we find that the significant contributions to the exponent are given by

$$st - \ell_0(s)z = \frac{\Delta t}{\kappa^2z^2}\sigma - 2\sigma^{1/2} \tanh\left(\frac{v}{\kappa z}\sigma^{1/2}\right) + \frac{\sigma^2}{48\kappa^4z^3} + O\left(\frac{1}{z}, \frac{1}{\kappa^2z^2}, \frac{1}{\kappa^6z^5}\right), \quad (2.19)$$

when Δt is comparable with κ^2z^2 , provided that $\kappa z, z \gg 1$. (Note that the κ'^2zs term in (2.18) is of order z^{-1} with this scaling.)

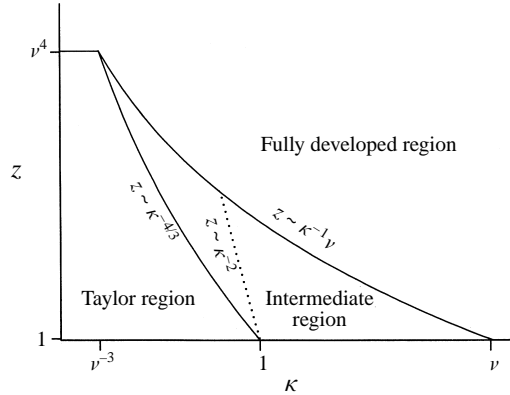


FIGURE 1. Schematic illustration of the regions of applicability of different approximations for the tracer concentration transient in the (κ, z) -plane. The character of the transient is determined by the size of z relative to the values $z_u = \max(1, \kappa^{-4/3})$ and $z_d = \kappa^{-1}\nu$. The Taylor region, for which $1 \ll z \ll \min(z_u, \nu^4)$ (for $\kappa \ll 1$), is treated in §3.2. The intermediate region, for which $z_u \ll z \ll z_d$ (for $\nu^{-3} \ll \kappa \ll \nu$), is treated in §3.1. (In the left-hand part of this region, where $z \ll \kappa^{-2}$ (for $\nu^{-3} \ll \kappa \ll 1$), the early approximation (3.3) is valid.) The fully developed region, for which $z \gg \min(z_d, \nu^4)$ (for $\kappa \ll \nu$) and $z \gg 1$ (for $\kappa \gg \nu$), is treated in §3.3.

3. Asymptotic approximations for the concentration transient

All the approximations considered in this paper require that the dimensionless downstream distance z be large. In addition, for a given value of κ in the range $\nu^{-3} \ll \kappa \ll \nu$, the character of the transient is found to depend on the size of z relative to the values $z_u = \max(1, \kappa^{-4/3})$ and $z_d = \kappa^{-1}\nu$. The regions of (κ, z) -space defined by these criteria are shown schematically in figure 1. Within each of the regions (and asymptotically far from their boundaries), the form of the main part of the concentration transient is particularly simple (see (3.1), (3.8) and (3.12) below). Near the boundaries between them, the behaviour is more complicated, reflecting the transitions between the different regimes. In addition, in each case the approximate solution breaks down at both short and long times. Table 1 (§5) shows the ranges of temporal validity of the approximate solutions presented in this section.

3.1. The intermediate region

Initially, we consider the intermediate range of axial distances defined by $z_u \ll z \ll z_d$. The mathematical details of the evaluation of the integral in (2.16), using the series expansion (2.18), are given in Appendix A.

The main part of the transient corresponds to values of Δt comparable with $\kappa^2 z^2$. The first two terms of (2.18) are dominant, with the hyperbolic tangent in the definition of κ' approximately equal to unity. In physical terms, this means that the character of the transient is determined by tracer exchange with a thin region of the wall layer adjacent to the interface. The flow profile and the presence of the outer boundary of the wall layer do not affect the solution at the leading order. The main part of the concentration transient is described by the skewed approximation

$$G(\mathbf{r}, z, t; \mathbf{r}_0) \sim \frac{\kappa z}{\pi^{1/2} \Delta t^{3/2}} \exp\left(-\frac{\kappa^2 z^2}{\Delta t}\right) \quad \text{for } \Delta t > 0 \quad (3.1)$$

(Appendix A, §A.1). In this approximation it is straightforward to obtain the corresponding solution for the tracer concentration within the wall layer. When \mathbf{r} lies

within the wall layer (but the point of release r_0 is in the fluid phase, as above), we find that

$$G(r, z, t; r_0) \sim \frac{\beta(\kappa z + \frac{1}{2}\lambda^{-1/2}[r-1])}{\pi^{1/2}\Delta t^{3/2}} \exp\left(-\frac{(\kappa z + \frac{1}{2}\lambda^{-1/2}[r-1])^2}{\Delta t}\right) \quad \text{for } \Delta t > 0. \quad (3.2)$$

(This approximation breaks down in the thin outermost region of the wall layer, where the distance from the outer boundary, relative to the thickness of the layer, is comparable with the small quantity $\kappa z/v$. The concentration is exponentially small in this region.) This solution can trivially be integrated with respect to r , to obtain the total quantity of tracer within the wall layer as a function of z and t ; this integrated result is equal, at leading order, to Young's (1988) equation (3.17), which was derived using a simplified model.

The approximations just given are not uniformly asymptotic: in Appendix A, their range of temporal validity is shown to be $\max(\kappa^2 z^{3/2}, \kappa z^{5/4}) \ll \Delta t \ll v^2$. The behaviour at earlier and later times is considered in the remainder of this subsection. In the approximation of (3.1) and (3.2), the concentration is zero for values of t less than z . In fact, the first arrival of tracer corresponds to advection with the peak velocity at the centreline, and occurs at $t = \frac{1}{2}z$. For values of Δt comparable with $\max(\kappa^2 z^{3/2}, \kappa z^{5/4})$ or smaller, (3.1) loses its validity, although at these early times the tracer concentration is exponentially small. The nature of the transient at earlier times depends on the values of κ and z , but a simple approximation may be found if the additional condition $z \ll \kappa^{-2}$ is imposed (this is possible if $\kappa \ll 1$; the corresponding region of (κ, z) -space is illustrated schematically in figure 1). As shown in Appendix A, §A.2, in this case the first, second and fourth terms of (2.18) are significant. Physically, this means that in addition to exchange with a thin region of the wall layer, the influence of the non-uniform velocity profile is important. The resulting approximation is

$$G(r, z, t; r_0) \sim \frac{1}{[\pi(\frac{1}{12} + \alpha^{-3})z]^{1/2}} \exp(-\kappa^{4/3}z(\frac{1}{48}\alpha^4 + \alpha)), \quad (3.3)$$

where α satisfies the cubic equation

$$\frac{1}{24}\alpha^3 + \frac{\Delta t}{\kappa^{2/3}z}\alpha - 1 = 0. \quad (3.4)$$

This approximation is valid (provided that $z \ll \kappa^{-2}$) for positive values of Δt up to order $\kappa z^{5/4}$, and for negative values with $|\Delta t|$ up to order $z^{2/3}$. In addition, it is easy to verify that for larger (positive) values of Δt , (3.3) tends towards the skewed form (3.1).

As well as breaking down at small times, the skewed approximation (3.1) behaves in a clearly unphysical manner at large times, when it predicts a slow, algebraic decay. As pointed out by Phillips *et al.* (1995), the consequence is that all the moments of the approximation (3.1) (beyond the zeroth) are infinite. In practice, the influence of the impermeable outer boundary eventually causes absorbed tracer to move back into the fluid phase more quickly, forcing a faster decay of the concentration tail. If this is taken into account, the temporal moments are seen to be finite, but much larger than a naive scaling argument based on (3.1) would suggest. In mathematical terms, the evaluation of the concentration when Δt is of order v^2 or larger requires the individual treatment of the singularities of the hyperbolic tangent along the negative real axis

of the s -plane. The details are given in Appendix A, §A 3, where it is demonstrated that the contribution of the m th singularity to G is given by (A 9). Thus we obtain

$$G(\mathbf{r}, z, t; \mathbf{r}_0) \sim \pi \left(\frac{\kappa z}{v^3 \Delta t} \right)^{1/2} e^{-3\kappa z/v} \sum_{m=0}^{\infty} (2m+1) I_1(a_m) e^{-b_m}, \quad (3.5)$$

in which I_1 is a modified Bessel function of the first kind, and the arguments a_m and b_m are given by

$$a_m = 2(2m+1)\pi \left(\frac{\kappa z \Delta t}{v^3} \right)^{1/2}, \quad b_m = \frac{(2m+1)^2 \pi^2 \Delta t}{4v^2}. \quad (3.6)$$

Combination of the conditions (A 7) with (A 8) shows that the temporal range of validity of this approximation is $\kappa v z \ll \Delta t \ll \kappa^{-1} v^3$.

The large-time approximation may be further simplified in parts of this temporal range, because in the intermediate region $\kappa z/v \ll 1$. Thus, we find that: (i) for $\Delta t \lesssim v^2$, the modified Bessel functions may be replaced by their (linear) small-argument approximations, and for $\Delta t \ll v^2$ this shows the series to be a discrete approximation to the integral form of (3.1), so that this solution joins smoothly on to the skewed form; (ii) for $\Delta t \gg v^2$, all terms but the leading one are negligible; (iii) at even larger times, $\Delta t \gg \kappa^{-1} v^3 z^{-1}$, the modified Bessel function may be replaced by its (exponential) large-argument approximation, although by this time the concentration is extremely small. (Note that at even larger times, when Δt becomes comparable with $\kappa^{-1} v^3$, the concentration becomes radially non-uniform in the fluid phase, and the expansion (2.18) is no longer valid.)

3.2. The upstream transition zone and the Taylor region

As well as breaking down at very early times within the intermediate region, (3.1) loses its validity during the main part of the transient as the boundary $z = z_u$ is approached. In the range $1 \lesssim \kappa \ll v$, this means that the dimensionless downstream distance z drops to order unity, which implies that there is insufficient time for radial equilibration of the concentration within the fluid, and the expansion (2.18) is not valid. However, for smaller values of κ ($v^{-3} \ll z \ll 1$), the upstream boundary of the intermediate region occurs when z is comparable with $\kappa^{-4/3}$ ($\gg 1$), and the expansion remains applicable. This is a zone of transition, in which the character of the concentration transient changes. It is clear from (2.19) that in this zone, where $\kappa^{4/3} z$ is of order unity, the σ^2 term becomes important (although – provided $\kappa \gg v^{-3}$ – the hyperbolic tangent may still be replaced by unity, and the error terms remain small). Placing the integration contour along the imaginary axis, we therefore obtain

$$G(\mathbf{r}, z, t; \mathbf{r}_0) \sim \frac{1}{\pi \kappa^2 z^2} \int_0^{\infty} \operatorname{Re} \left[\exp \left\{ \frac{\Delta t}{\kappa^2 z^2} \sigma - 2\sigma^{1/2} + \frac{\sigma^2}{48 \kappa^4 z^3} \right\} \right]_{\sigma=iu} du. \quad (3.7)$$

The presence of the σ^2 term means that in general this integral must be evaluated numerically. As illustrated by the numerical results in §4, this solution tends towards the early approximation (3.3) at small times, and towards the skewed approximation (3.1) at large times.

If we now move upstream of the transition zone (for $v^{-3} \ll \kappa \ll 1$), to consider distances such that $1 \ll z \ll \kappa^{-4/3}$ (see figure 1), the approximation (3.7) simplifies. The σ^2 term in the exponent causes the integrand to decay over the small scale $\kappa^2 z^{3/2}$, and the $\sigma^{1/2}$ term in the exponent becomes negligible. The resulting integral may be evaluated explicitly using Gradshteyn & Ryzhik (1980, eqn 3.896.4), to give the

simpler approximation

$$G(\mathbf{r}, z, t; \mathbf{r}_0) \sim \left(\frac{12}{\pi z}\right)^{1/2} \exp\left(-\frac{12\Delta t^2}{z}\right), \quad (3.8)$$

which is simply the temporal counterpart of Taylor's Gaussian approximation for the tracer concentration distribution in the absence of a wall layer. This demonstrates that, for small values of the absorption parameter κ , there exists a range of distances over which Taylor dispersion has developed, but the influence of the wall layer on the main part of the concentration transient may be neglected. (In fact, it may be shown directly from (2.18) that (3.8) is also valid for extremely small values of κ ($\lesssim v^{-3}$), provided that $z \ll v^4$; see figure 1.)

The Gaussian approximation (3.8) breaks down at very small times, when either the s^3 or the $s^{1/2}$ term in (2.18) becomes significant. This corresponds to negative values of Δt , with $|\Delta t|$ comparable with $\min(z^{2/3}, \kappa^{-2}z^{-1})$. At large times the situation is complicated by the presence of the branch cut in the s -plane. In this case the approximation is found to fail when Δt becomes comparable with $\min(z^{2/3}, z^{1/2}|\ln(\kappa z^{3/4})|^{1/2})$. If the logarithmic time-scale is reached first, the Gaussian approximation is supplanted at large times by the skewed form (3.1).

3.3. The downstream transition zone and the fully developed region

The downstream boundary of the intermediate region, where z becomes comparable with $z_d = \kappa^{-1}v$, is another zone of transition, where the skewed approximation (3.1) breaks down, because the hyperbolic tangent in (2.19) may no longer be approximated by unity. Physically, this means that the impermeable condition at the outer boundary of the wall layer becomes significant. In this zone (which covers the range $v^{-3} \ll \kappa \ll v$), the third and error terms in (2.19) remain small compared with unity. Once again, placing the integration contour along the imaginary axis, we obtain

$$G(\mathbf{r}, z, t; \mathbf{r}_0) \sim \frac{1}{\pi \kappa^2 z^2} \int_0^\infty \operatorname{Re} \left[\exp \left\{ \frac{\Delta t}{\kappa^2 z^2} \sigma - 2\sigma^{1/2} \tanh \left(\frac{v}{\kappa z} \sigma^{1/2} \right) \right\} \right]_{\sigma=i u} du. \quad (3.9)$$

In general this integral, like that in (3.7), must be evaluated numerically. As illustrated by the numerical results in §4, this solution tends towards the skewed approximation (3.1) at small times, and towards the late approximation (3.5) at large times.

If we move still further downstream, so that z becomes much larger than z_d , the approximation (3.9) simplifies. In mathematical terms, the argument of the hyperbolic tangent becomes small, and it is appropriate to expand in powers of $\sigma^{1/2}$. We find that the resulting σ^2 term causes the integrand to decay over the scale $(\kappa v^{-1}z)^{3/2}$, so that the only significant terms in the exponent are proportional to σ and σ^2 . Thus, as in the last subsection, we obtain a simpler Gaussian approximation for the tracer concentration transient. Physically, the radial tracer distribution has become almost uniform over both the fluid phase and the wall layer. There has been sufficient distance for the full development of the analogue of Taylor dispersion in the two-phase system, resulting in a Gaussian distribution whose mean and variance are both influenced by the properties of the wall layer.

This Gaussian approximation may also be found from an alternative series solution of the eigenvalue problem (2.10a), (2.12), applicable for very small values of s ($\ll \min(v^{-2}, \kappa^{-1}v^{-1})$), obtained by expanding \tanh in powers of $s^{1/2}$. This derivation makes it clear that neither the condition $v^{-3} \ll \kappa \ll v$ nor the assumption that v is large is necessary at this stage. For generality, the equations given below do not

rely on these assumptions (if v were large, the term proportional to κv would be negligible). In this manner, we obtain a series approximation for $\ell_0(s)$ in integral powers of s , which gives

$$st - \ell_0(s)z = (t - M)s + \frac{1}{2}S^2s^2 + O(1, \kappa^3v^3, \kappa v^5)zs^3, \quad (3.10)$$

where the coefficients M and S^2 are given by

$$M = (1 + 2\kappa v)z, \quad S^2 = \left(\frac{1}{24} + \frac{1}{2}\kappa v + \frac{11}{6}\kappa^2v^2 + \frac{4}{3}\kappa v^3\right)z. \quad (3.11)$$

It is found that, in evaluating the integral (2.16), the error terms in (3.10) are negligible provided that $t - M$ scales as S , and that z is sufficiently large. The precise condition on z depends on the value of κ . In the range $v^{-3} \ll \kappa \ll v$, it is that $z \gg z_d$. For smaller values ($\kappa \lesssim v^{-3}$), it is sufficient that $z \gg v^4$, and for larger values ($\kappa \gtrsim v$), that $z \gg 1$. The corresponding region of (κ, z) -space is illustrated in figure 1. Thus we obtain the ‘fully developed’ Gaussian approximation for the Green’s function

$$G(\mathbf{r}, z, t; \mathbf{r}_0) \sim \frac{1}{(2\pi)^{1/2}S} \exp\left(-\frac{(t - M)^2}{2S^2}\right). \quad (3.12)$$

This approximation is the temporal counterpart of the Gaussian axial distribution found by Golay (1958). The range of temporal validity of this approximation, which may be determined by considering the size of the neglected terms in (3.10) at the saddle point, also depends upon the value of κ . For the main part of the region ($v^{-3} \ll \kappa \ll v$), the approximation breaks down when $|t - M|$ becomes comparable with $(\kappa v^2 z)^{2/3}$.

Finally, note that the upstream and downstream transitional zones meet at the tip of the intermediate region, where κ is comparable with v^{-3} , and z with v^4 (see figure 1). In this regime, the full expression (2.19) (excluding the error terms) must be incorporated in an integral similar to (3.7) or (3.9), giving a rather more complicated result, which once again must be determined numerically.

4. Numerical results

In this section, numerical results are given, to illustrate the relationship between the simple asymptotic approximations (3.1), (3.8) and (3.12), valid in different regions of (κ, z) -space, and the transitional forms (3.7) and (3.9), applicable near the boundaries of these regions (see figure 1). In presenting the results, it will be convenient to use three rescalings, based on the characteristic concentration and time scales of the three simple approximations. Note that each of the rescalings preserves the integral of concentration with respect to time; in physical terms this is proportional to the total amount of tracer advected past the observation point, which means that the area under each curve shown in this section is the same (and is equal to unity).

Near the upstream boundary of the intermediate region, there is a transition between the Taylor Gaussian form, for which the effect of the wall layer is negligible, and the skewed approximation, for which it is dominant. First, we examine the way in which the upstream transitional form (3.7) departs from the Taylor Gaussian approximation (3.8). To illustrate this, it is convenient to use a rescaling based on the concentration and time scales of the Gaussian, that is, to plot $z^{1/2}G$ against $z^{-1/2}\Delta t$. With this rescaling, the transitional form depends on the single dimensionless parameter $\kappa^{4/3}z$ (which, in the transitional zone, expresses the ratio of z to z_u), and tends towards the Gaussian as $\kappa^{4/3}z \rightarrow 0$. In figure 2, this rescaling is employed to

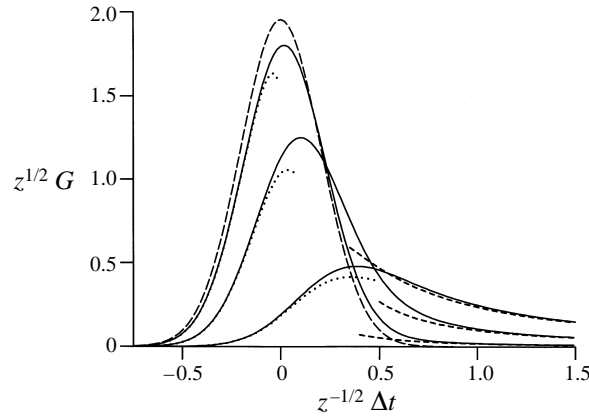


FIGURE 2. Graph showing $z^{1/2}G$ plotted against $z^{-1/2}\Delta t$, to illustrate the departure of the upstream transitional form (3.7) from the Taylor Gaussian approximation (3.8), as $\kappa^{4/3}z$ increases. ---, Gaussian approximation; —, upstream transitional form, for $\kappa^{4/3}z = 10^{-2}$, 10^{-1} and $\frac{1}{2}$, in order of decreasing peak height; early approximation (3.3); - - -, skewed approximation (3.1).

plot the Gaussian approximation, and the transitional form for $\kappa^{4/3}z = 10^{-2}$, 10^{-1} and $\frac{1}{2}$. These curves may be thought of as describing the concentration transient either at successively larger downstream distances, or for larger values of the absorption parameter κ (implying larger partition coefficients or diffusivities within the wall layer). The results illustrate the departure of the transient from the Gaussian form, even for quite small values of $\kappa^{4/3}z$, characterized by a substantial reduction in the peak concentration (by 10% when $\kappa^{4/3}z$ is about 0.014, and to about two thirds of the Gaussian value by $\kappa^{4/3}z = 10^{-1}$). The temporal location of the peak changes more gradually, and the main part of the curve retains a fairly 'Gaussian' appearance. However, the decrease in concentration during the main part of the transient is compensated by the formation of a long, gradually decaying tail, so that the area under each curve remains equal to unity. Its form is described by the skewed approximation (3.1), which for the cases shown becomes virtually indistinguishable from the numerical values beyond $z^{-1/2}\Delta t = 1$. The tail accounts for a significant fraction of the area under the curve, and causes the temporal moments of concentration (beyond the zeroth) to be infinite. Awareness of this behaviour may be very important in practice, especially if the presence of noise makes the accurate measurement of concentration difficult. Also shown in figure 2 is the early approximation (3.3), which in each case describes the early part of the transient closely, but loses accuracy before the peak is reached.

While the transitional solution (3.7) departs from the Taylor Gaussian as $\kappa^{4/3}z$ increases, it approaches the skewed form given by (3.1). To illustrate this, we use a rescaling based on the concentration and time scales appropriate in the intermediate region, that is, we plot $\kappa^2 z^2 G$ against $\kappa^{-2} z^{-2} \Delta t$. This means that the transitional form again depends only on $\kappa^{4/3}z$, and tends towards the skewed approximation as $\kappa^{4/3}z \rightarrow \infty$. In figure 3, this rescaling is used to show results for $\kappa^{4/3}z = \frac{1}{5}$, $\frac{1}{2}$ and 1, together with the skewed approximation and the early approximation (note that the values of $\kappa^{4/3}z$ represented here are somewhat larger than those in figure 2). The limiting process illustrated here is the converse of that shown in figure 2: a transient with a broadly 'Gaussian' appearance becomes more sharply peaked and less symmetrical, as either the distance z or the absorption parameter κ increases. As

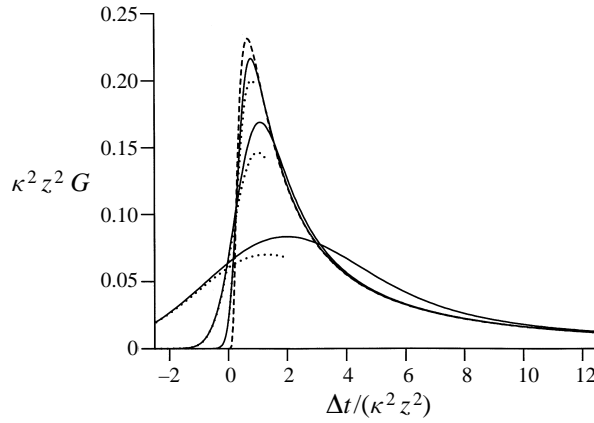


FIGURE 3. Graph showing $\kappa^2 z^2 G$ plotted against $\kappa^{-2} z^{-2} \Delta t$, to illustrate the approach of the upstream transitional form (3.7) to the skewed approximation (3.1), as $\kappa^{4/3} z$ increases. - - -, skewed approximation; —, upstream transitional form, for $\kappa^{4/3} z = \frac{1}{5}, \frac{1}{2}$ and 1, in order of increasing peak height; ·····, early approximation (3.3).

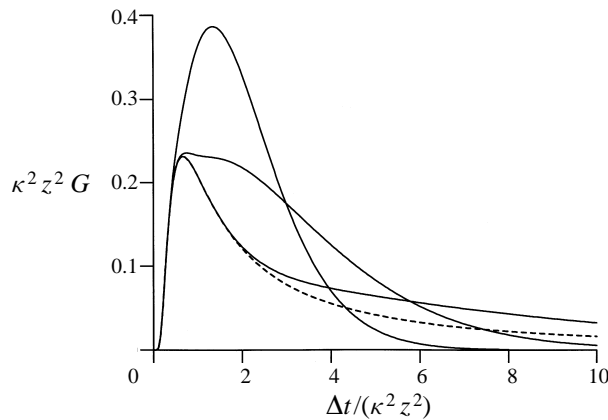


FIGURE 4. Graph showing the main part of the transient $\kappa^2 z^2 G$ plotted against $\kappa^{-2} z^{-2} \Delta t$, to illustrate the departure of the downstream transitional form (3.9) from the skewed approximation (3.1), as $\kappa v^{-1} z$ increases. - - -, skewed approximation; —, downstream transitional form, for $\kappa v^{-1} z = \frac{1}{3}, \frac{2}{3}$ and 1, in order of increasing peak height.

already seen, the large-time tail agrees closely with the skewed form even for relatively small values of $\kappa^{4/3} z$. Near the beginning of the transient, we see that, as the skewed form is approached, there is a decrease in the amount of tracer arriving in $\Delta t < 0$, and a compensatory increase in the height of the peak immediately afterwards. By about $\kappa^{4/3} z = 0.84$ the peak has reached 90% of the value predicted by (3.1).

At the downstream boundary of the intermediate region, a different transition occurs, between the skewed approximation, for which the influence of the outer boundary of the wall layer is small, and the fully developed Gaussian form, in which tracer has equilibrated across the wall layer. In figures 4 and 5, we illustrate the way in which the transient departs from the skewed form as we move downstream. With the same rescaling as in figure 3, the downstream transitional form (3.9) depends only on the dimensionless parameter $\kappa v^{-1} z$ (which expresses the ratio of z to z_d), and tends towards the skewed approximation (3.1) as $\kappa v^{-1} z \rightarrow 0$. In figure 4, the main part of

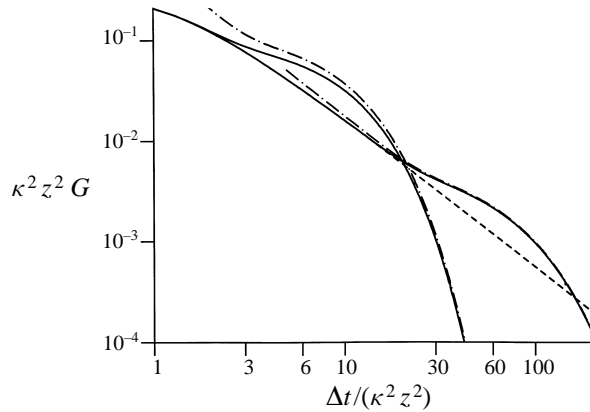


FIGURE 5. Logarithmic plot to show the late transient of $\kappa^2 z^2 G$ plotted against $\kappa^2 z^{-2} \Delta t$, illustrating the relationship between the downstream transitional form (3.9) and the skewed approximation (3.1), for small values of $\kappa v^{-1} z$. - - -, skewed approximation; —, downstream transitional form, for $\kappa v^{-1} z = \frac{1}{10}$ and $\frac{1}{3}$; the latter of these diverges earlier from the skewed approximation; - · - ·, late approximation (3.5).

the transient is shown for $\kappa v^{-1} z = \frac{1}{3}, \frac{2}{3}$ and 1. For the smallest value, the computed curve follows the skewed approximation closely as far as the peak and for some way beyond it, but thereafter the concentration in the tail rises to as much as twice that predicted by (3.1). Physically, this is because the impermeable outer boundary of the wall layer stops the outward diffusion of tracer, causing it to return to the fluid phase and to reach the point of observation earlier than it would otherwise have done. The behaviour of the $\kappa v^{-1} z = \frac{1}{3}$ curve at larger times is shown in a logarithmic plot in figure 5. The earlier excess of concentration is compensated by a subsequent fall of concentration below the value predicted by the skewed approximation. This process is described quite closely by the late approximation (3.5): thus the influence of the outer boundary eventually induces an exponential, rather than an algebraic, decay of the concentration. As a result, the temporal moments of concentration are finite, although they primarily reflect the characteristics of the tail, rather than the main part of the transient where the concentration is higher. Also shown in figure 5 is the transient for the smaller value $\kappa v^{-1} z = \frac{1}{10}$, which behaves similarly, but diverges from the skewed approximation at a later period. This divergence, and the subsequent decay, are accurately described by the late approximation (3.5).

Returning to the main part of the transient shown in figure 4, we see that for larger values of $\kappa v^{-1} z$, both the rise in concentration above that predicted by (3.1) and the following decay occur progressively earlier, giving rise first to a pronounced 'hump' following the peak, and then to a dramatic increase in the height of the peak, followed by a prompt decay of concentration. By about $\kappa v^{-1} z = 0.73$ the peak has risen to 10% above that predicted by (3.1), although by then the shape of the curve as a whole is very different.

Finally, we consider the approach of the downstream transitional form (3.9) to the fully developed Gaussian approximation, which occurs at large distances. Although the transient approaches the Gaussian form (3.12) at sufficiently large z for any value of v , here we restrict our attention to the range $v^{-3} \ll \kappa \ll v$, which corresponds to the downstream boundary of the intermediate region. In this range, the variance of the Gaussian, defined by (3.11), may be approximated by $S^2 \sim \frac{4}{3} \kappa v^3 z$. Based on the concentration and time scales of the resulting Gaussian, we plot $(\kappa v^3 z)^{1/2} G$

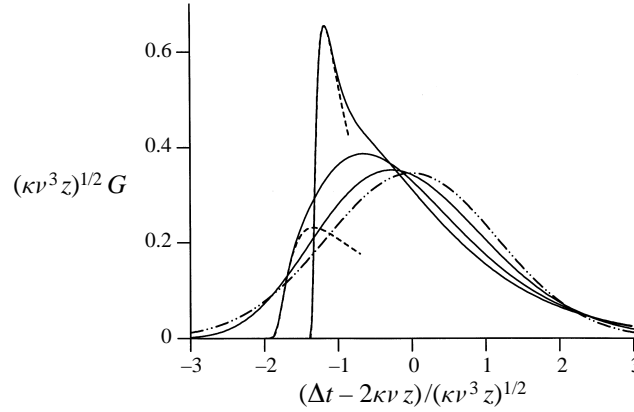


FIGURE 6. Graph showing $(\kappa v^3 z)^{1/2} G$ plotted against $(\kappa v^3 z)^{-1/2} (\Delta t - 2\kappa v z)$, to illustrate the approach of the downstream transitional form (3.9) to the large-distance Gaussian approximation (3.12) (for $v^{-3} \ll \kappa \ll v$), as $\kappa v^{-1} z$ increases. $\cdots\cdots$, Gaussian approximation; — , downstream transitional form, for $\kappa v^{-1} z = \frac{1}{2}, 1$ and 5 , in order of decreasing peak height; \cdots , skewed approximation (3.1).

against $(\kappa v^3 z)^{-1/2} (\Delta t - 2\kappa v z)$: with such a rescaling, the downstream transitional form depends only on the parameter $\kappa v^{-1} z$, and tends towards the fully developed Gaussian as $\kappa v^{-1} z \rightarrow \infty$. In figure 6 we show the transitional form for $\kappa v^{-1} z = \frac{1}{2}, 1$ and 5 , together with the Gaussian. The main features of the limiting process are that the peak becomes broader and lower, and occurs later in time, approaching $\Delta t = 2\kappa v z$, while the transient as a whole becomes more symmetrical. The peak concentration drops quite rapidly towards the Gaussian value, lying within 10% of it by about $\kappa v^{-1} z = 1.14$, but the approach of the temporal position of the peak is more gradual. The skewed approximation (3.1), which describes the early part of the transient, is also shown, although its usefulness is clearly limited beyond about $\kappa v^{-1} z = 1$.

5. Discussion and applications

In this paper, we have considered the development of dispersion in a system in which a tracer substance is exchanged between a flowing phase and a fixed phase, in which its diffusivity is much smaller. The problem has been formulated in terms of the temporal variation of concentration at a fixed axial position, following the initial release of tracer at some point within the fluid. Rather than attempting to solve the governing equations numerically, we have adopted an analytic approach based on asymptotic approximations. This has the virtue of identifying clearly the important governing parameters, together with the different possible regimes of behaviour and the physical mechanisms which are dominant. The crucial assumption, necessary to allow analytic progress to be made, is that the diffusivity within the fixed phase is sufficiently small that diffusion across it takes much longer than diffusion across the fluid. This means that approximate solutions for the tracer concentration may be found at distances smaller than those required for the full development of dispersion, which eventually produces a Gaussian concentration distribution (Golay 1958). However, the tracer is assumed to have equilibrated within the fluid phase, which implies that the measured concentration is insensitive to both the radial position at which it is observed, and the initial radial distribution of tracer within the fluid.

The character of the transient is found to be governed by three dimensionless parameters: the downstream distance z , defined in (2.5), the absorption parameter κ ,

Approximation	Temporal range of validity
Taylor region	
Taylor Gaussian: equation (3.8)	$t - z < 0 : t - z \ll \min(z^{2/3}, \kappa^{-2}z^{-1});$ $t - z \geq 0 : t - z \ll \min(z^{2/3}, z^{1/2} \ln(\kappa z^{3/4}) ^{1/2})$
Intermediate region	
Early part: equation (3.3) (provided that $z \ll \kappa^{-2}$)	$t - z < 0 : t - z \ll z^{2/3};$ $t - z \geq 0 : t - z \lesssim \kappa z^{5/4}$
Skewed approximation: equation (3.1)	$\max(\kappa^2 z^{3/2}, \kappa z^{5/4}) \ll t - z \ll v^2$
Late part: equation (3.5)	$\kappa v z \ll t - z \ll \kappa^{-1} v^3$
Fully developed region	
Golay Gaussian: equation (3.12)	$ t - z - 2\kappa v z \ll (\kappa v^2 z)^{2/3} \quad (\text{for } v^{-3} \ll \kappa \ll v)$

TABLE 1. Summary of approximations and their temporal ranges of validity

and the effective wall layer thickness v , both defined in (2.13). (Of these parameters, z and v are large by assumption.) In terms of (κ, z) parameter space, there exist three regions, which are illustrated schematically in figure 1. These regions differ according to the importance of the effect of the wall layer during the main part of the concentration transient. In the first region shown, the wall layer has only a small influence, so that the transient is described approximately by the Taylor Gaussian (3.8). In the intermediate region, absorption is significant, but the presence of the outer boundary of the wall layer has little effect. The result is the characteristic skewed variation of concentration with time (3.1). In the third region, tracer concentration has had time to become almost uniform over the cross-section, including the wall layer. As a result the transient is described approximately by the Golay Gaussian (3.12). Near the boundaries between these regions in (κ, z) -space are zones of transition, where the integral forms (3.7), (3.9) apply.

The three simple solutions referred to above describe only the main part of the concentration transient in each region; the precise ranges of temporal validity are given in table 1. They are also illustrated in figure 7, where the corresponding regions in the $(t - z, z)$ -plane are shown schematically for two ranges of the parameter κ . In each case, the simple approximation breaks down both near the onset of the transient and at very large times. However, in the intermediate region of (κ, z) -space, relatively simple approximations may also be available for the behaviour of the tail at earlier and later times. For at least part of the parameter range (as shown in figure 7a), the early part of the transient is described by (3.3): this behaviour is influenced both by the slight non-uniformity of the radial tracer distribution in the fluid phase, and by the small amount of tracer absorption by the wall layer. The later part of the transient, in which the outer boundary of the wall layer becomes important, satisfies (3.5).

It is useful to re-express in dimensional terms the criteria defining the intermediate region, where the skewed approximation applies. In terms of the partition coefficient β and the axial distance Z , the required conditions are that

$$\frac{D_w a^3}{D h^3} \ll \beta \ll \frac{D h}{D_w a}, \quad \max\left(\frac{V_m a^2}{D}, \frac{V_m a^2}{(\beta^4 D D_w^2)^{1/3}}\right) \ll Z \ll \frac{V_m a h}{\beta D_w}. \quad (5.1)$$

Although derived in this paper for a specific flow profile and geometry, and with the

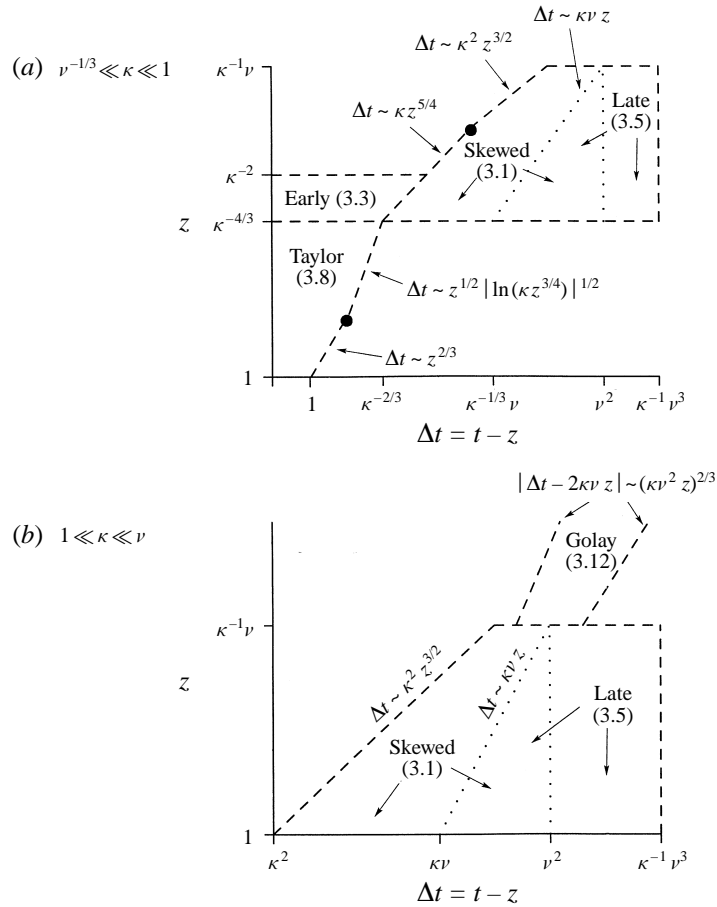


FIGURE 7. Schematic illustrations of the temporal ranges of validity of the approximate solutions. Axial distance z is plotted against the time difference $\Delta t = t - z$, for two ranges of κ . (a) For $\nu^{-1/3} \ll \kappa \ll 1$, the distance-time plane is shown for $1 \ll z \ll \kappa^{-1}\nu$ and $\Delta t \gg 1$. (For $z \gg \kappa^{-1}\nu$, the behaviour is as shown in (b) below.) The behaviour is similar for smaller values of κ : for $\nu^{-1} \ll \kappa \ll \nu^{-1/3}$, the boundary segment $\Delta t \sim \kappa^2 z^{3/2}$ is absent; for $\nu^{-3} \ll \kappa \ll \nu^{-1}$, the early form (3.3) remains valid up to $z \sim \kappa^{-1}\nu$. (b) For $1 \ll \kappa \ll \nu$, the distance-time plane is shown for $z \gg 1$, $\Delta t \ll 1$. (For $\kappa \gg \nu$, the upper part of the diagram describes the behaviour over the whole range $z \gg 1$.)

assumption of infinite Péclet number, the skewed approximation is expected to be applicable to a range of related systems. In Appendix B it is demonstrated explicitly that the assumptions that the Péclet number is infinite and that the wall layer is thin are unnecessary for its validity. In fact, it is clear from the derivation that, provided the absorption parameter κ is defined with reference to the surface area per unit length of the pipe, it is not even necessary that the cross-section be circular: the dimensional form of the approximation in this case is given by (B 6). Similarly, by an appropriate definition of κ , it may also be applied to systems which are not axially invariant, such as columns packed with permeable beads (cf. Reis *et al.* 1979).

Most of the other approximate solutions presented here may also be extended to other geometries, with more or less effort. Thus, it is clear from the working of §2 (leading to (2.19)) that a suitably rescaled version of the upstream transitional

form (3.7) will be more generally applicable, provided that the coefficient of the σ^2 term is fixed with reference to the dispersion coefficient which would apply in the absence of absorption by the wall layer. Knowledge of this coefficient also allows the early approximation analogous to (3.3) to be written down immediately. (Of course, this dispersion coefficient may itself not be trivial to calculate.) The downstream transitional form (3.9) may also be generalized, but a little more work is required here, because the hyperbolic tangent is specific to the (thin) annular geometry of the wall layer. What is required instead, following the reasoning of §§2, 3, is to define a function g within the fixed phase, satisfying $\nabla_r^2 g = \lambda^{-1} s g$, subject to the boundary condition $g = 1$ at the interface. Then in (2.12), the quantity $\kappa' s^{1/2}$ must be replaced by the average value, over the interface, of $\beta \lambda \partial g / \partial n$ (where $\partial / \partial n$ denotes the normal derivative). Once this replacement function has been defined, we may deduce not only the downstream transitional form (by numerical integration), but also the late approximation analogous to (3.5) (by examining the singularities of the function), and the fully developed Gaussian approximation corresponding to (3.12) (by expanding the function for small values of s). Thus, as well as giving qualitative information about the behaviour of similar systems, in principle each of the approximations derived in this paper may be generalized in a precise manner.

C. G. P. is grateful to the Wellcome Trust for support from a Research Fellowship during the course of this work.

Appendix A. Inversion of the Laplace transform in the intermediate region

In this Appendix, we give mathematical details of the derivation of the three approximations (3.1), (3.3) and (3.5), presented in §3.1, which describe, respectively, the main, early and late parts of the concentration transient in the intermediate region. Using similar arguments it may be shown that (3.3) also describes the early transient in the upstream transition zone, and that (3.5) also describes the late transient in the downstream transition zone (see figure 1).

We have previously considered the development of shear dispersion in a system similar to the present one, but without an absorbing wall layer (Phillips & Kaye 1996). In this case, the exponent which appears in (2.16) has a single saddle point on the real axis of the s -plane, whose position depends on the value of t . The saddle point lies at $s = 0$ when $t = z$; it moves along the positive axis for smaller values of t (tending to ∞ as $t \rightarrow \frac{1}{2}z$) and along the negative axis for larger values of t (tending to $-\infty$ as $t \rightarrow \infty$). When z is large, the integral corresponding to (2.16) may be evaluated, at leading order, by using a quadratic approximation for the exponent in the neighbourhood of the saddle point. In the present problem, the behaviour of the exponent is different because, owing to the presence of the hyperbolic tangent in the boundary condition (2.12), there is an infinite sequence of singularities on the negative real axis, at $s = -\frac{1}{4}(2m+1)^2 \pi^2 v^{-2}$, for $m = 0, 1, 2, \dots$

A.1. The main part of the transient

We consider first the main part of the transient, for which Δt is comparable with $\kappa^2 z^2$. The exponent varies over the scale $\kappa^{-2} z^{-2}$ in the s -plane, and it is convenient to use the rescaled variable $\sigma = \kappa^2 z^2 s$. With this scaling, we find that all but the first two terms of the expansion (2.19) are small compared with unity, and that the hyperbolic

tangent may be replaced by unity. Thus we have

$$G(\mathbf{r}, z, t; \mathbf{r}_0) \sim \frac{1}{2\pi i \kappa^2 z^2} \int_{\mathcal{C}_0} \exp\left(\frac{\Delta t}{\kappa^2 z^2} \sigma - 2\sigma^{1/2}\right) d\sigma. \quad (\text{A } 1)$$

In this approximation, the exponent has a saddle point, whose position is given by

$$\sigma \sim \frac{\kappa^4 z^4}{\Delta t^2}. \quad (\text{A } 2)$$

The scale on which the exponent varies along the integration contour is comparable with the distance of the saddle point from the origin, and much larger than the spacing of the singularities along the negative real axis. Setting the hyperbolic tangent equal to unity is equivalent to the replacement of these singularities by a branch cut. The integral may conveniently be evaluated by deforming the contour around the negative real axis, and then using Gradshteyn & Ryzhik (1980, eqn 3.952.1), to obtain (3.1).

In this regime, it is easy to obtain the corresponding approximation for the concentration distribution within the wall layer. When \mathbf{r} lies within the wall layer, in the definition (2.9) of the function F_0 , the function $f_0(\mathbf{r}; s)$ is given by (2.11), but the remainder is unchanged. In the fluid phase we still have $f_0 \sim 1$, so that the quantity $A_0(s)$ can be determined directly from the second boundary condition of (2.2). Finally, we note that the scaling assumptions for the intermediate region imply that the argument of cosh in (2.11) is large, so that it can be approximated by an exponential (except very near the outer boundary, where $1 + \epsilon - r$ is asymptotically small). The result is that the integrand in (2.8) is as for the fluid phase, but with κz replaced by $\kappa z + \frac{1}{2}\lambda^{-1/2}[r - 1]$. So the integral can be evaluated in exactly the same way as before, to give (3.2).

A.2. The early part of the transient

As Δt becomes smaller, the position of the saddle point given by (A 2) moves to the right along the real axis of the s -plane. Because s remains much larger than ν^{-2} , the hyperbolic tangent remains close to unity and, as above, κ' may be replaced by κ in (2.18). In the range $\max(\kappa^2 z, \kappa^{2/3} z) \ll \Delta t \ll \kappa^2 z^2$, we find that the position of the saddle point continues to be described by (A 2). Moreover, the integrand in (2.16) is significant only in a small neighbourhood of the saddle point, and a local quadratic approximation may be used to evaluate the integral. For the more restricted range of times $\max(\kappa^2 z^{3/2}, \kappa z^{5/4}) \ll \Delta t \ll \kappa^2 z^2$, this procedure gives the same approximation, (3.1), as already obtained by deforming the integration contour around the branch cut. At earlier times, even though the position of the saddle point is still given by (A 2), other terms of the exponent become important.

A convenient approximate solution for earlier times, valid in part of the intermediate region, may be obtained by making the additional assumption that $z \ll \kappa^{-2}$. In this case, the first additional term of the exponent (2.18) to become significant is the zs^2 contribution, which comes in when Δt falls to the order $\kappa z^{5/4}$. A balance is obtained between this and the first two terms when s is of order $\kappa^{2/3}$. With this scaling, the saddle point is found to lie, to leading order, at $s = \kappa^{2/3} \alpha^2$, where α satisfies the cubic equation (3.4). Forming the Taylor expansion of the exponent, we find (using (3.4) for some simplification) that

$$st - \ell_0(s)z = -\left(\frac{1}{48}\alpha^4 + \alpha\right)\kappa^{4/3}z + \frac{1}{4}\left(\frac{1}{12} + \alpha^{-3}\right)z \delta s^2 + O(\kappa^2 z, \kappa^{2/3} z \delta s^2, \kappa^{-2/3} z \delta s^3), \quad (\text{A } 3)$$

where δs denotes $s - \kappa^{2/3} \alpha^2$, the distance from the saddle point. The dominant contribution to the integral in (2.16) comes from small values of δs , of order $z^{-1/2}$.

With this scaling, and the assumption already made that $z \ll \kappa^{-2}$, the error terms are found to be small compared with unity. It therefore remains only to integrate the resulting Gaussian, which gives (3.3). This approximation remains valid down to times when Δt is negative and $|\Delta t|$ is comparable with $z^{2/3}$. At this and earlier times the zs^3 term in (2.18) becomes important (as it does in the absence of the wall layer).

A.3. The late part of the transient

When Δt rises to become comparable with v^2 , the scale of variation in the s -plane shrinks to v^{-2} . The hyperbolic tangent in (2.12) must be retained, and the singularities along the negative real axis must be treated individually, as follows. Suppose that the contour of integration is deformed, passing around the m th singularity as

$$s = -\xi_m + \eta_m e^{i\theta} \quad \text{where} \quad \xi_m = \frac{(2m+1)^2 \pi^2}{4v^2}, \quad (\text{A } 4)$$

for $0 \leq \theta < 2\pi$ and for $m = 0, 1, 2, \dots$. As $\eta_m \rightarrow 0$ this means that

$$\kappa' s^{1/2} \equiv \kappa s^{1/2} \tanh(v s^{1/2}) = -\frac{2\kappa \xi_m}{v \eta_m} e^{-i\theta} + \frac{3\kappa}{2v} + \dots \quad (\text{A } 5)$$

Under the conditions given by (A 7) below, the exponent (2.18) may therefore be approximated by

$$st - \ell_0(s)z = (-\xi_m + \eta_m e^{i\theta})\Delta t + \frac{4\kappa z \xi_m}{v \eta_m} e^{-i\theta} - \frac{3\kappa z}{v} + \dots \quad (\text{A } 6)$$

Note that, in the intermediate region, the final term is small. However, if it is retained here, this derivation may be applied also in the downstream transition zone (§ 3.3) for large times.

We know that in the intermediate region, $z \ll \min(\kappa^{-1}v, v^4)$ (see figure 1); we must also impose additional conditions on η_m to justify the use of the series expansions (2.14) and (A 5), and to ensure that the higher-order terms containing κ' are small. Combining these conditions, we require that

$$\kappa v^{-3} z^{1/2} \ll \eta_m \ll v^{-2}. \quad (\text{A } 7)$$

The approximation (A 6) implies that there is a local saddle point of the exponent, on the real axis just above the singularity, at

$$\eta_m = 2 \left(\frac{\kappa z \xi_m}{v \Delta t} \right)^{1/2} = (2m+1)\pi \left(\frac{\kappa z}{v^3 \Delta t} \right)^{1/2}. \quad (\text{A } 8)$$

With this choice of η_m , we find that the contribution to G from the m th singularity may be written

$$\begin{aligned} B_m &= \pi^{-1} \eta_m e^{-3\kappa z/v - \xi_m \Delta t} \int_0^\pi e^{2\eta_m \Delta t \cos \theta} \cos \theta \, d\theta \\ &= (2m+1)\pi \left(\frac{\kappa z}{v^3 \Delta t} \right)^{1/2} I_1 \left(2(2m+1)\pi \left(\frac{\kappa z \Delta t}{v^3} \right)^{1/2} \right) \exp \left(-\frac{3\kappa z}{v} - \frac{(2m+1)^2 \pi^2 \Delta t}{4v^2} \right), \end{aligned} \quad (\text{A } 9)$$

in which I_1 is a modified Bessel function of the first kind; the integral has been evaluated using Gradshteyn & Ryzhik (1980, eqn 3.387.1). This approximation is valid, with the argument of the modified Bessel function of order unity, when Δt is

comparable with $\kappa^{-1}v^3z^{-1}$, so that the radii η_m of the integration contours are of the order $\kappa z/v^3$. The resulting large-time series approximation for the concentration is given by (3.5).

Appendix B. The validity of the skewed approximation for smaller values of the Péclet number and in other geometries

We demonstrate that the skewed approximation remains valid, at leading order, in the intermediate region, if the assumptions concerning the Péclet number and the thinness of the wall layer are relaxed.

B.1. The skewed approximation when the Péclet number is finite

If we retain the axial diffusion term in (2.6) in the fluid phase (but assume that λ is sufficiently small that it may still be neglected in the wall layer), it is straightforward to show that the eigenvalue ℓ_0 in (2.14) is modified by the addition of a contribution

$$\ell_{0p} = m_{2p}s + m_{3p}s^{3/2} + m_{4p}s^2 + O(s^{5/2}), \quad (\text{B } 1)$$

where the coefficients m_{jp} are given by

$$\left. \begin{aligned} m_{2p} &= -4\kappa'^2 P^{-2}, \\ m_{3p} &= (-4\kappa' + \frac{14}{3}\kappa'^3)P^{-2} + 16\kappa'^3 P^{-4}, \\ m_{4p} &= (-1 + 4\kappa'^2 - \frac{2599}{720}\kappa'^4)P^{-2} + (24\kappa'^2 - \frac{91}{3}\kappa'^4)P^{-4} - 80\kappa'^4 P^{-6}. \end{aligned} \right\} \quad (\text{B } 2)$$

These additional terms result in a perturbation to the exponent in (2.16). In order that the skewed approximation remain valid at leading order in the intermediate region, we require that this perturbation be small compared with unity for values of s comparable with $\kappa^{-2}z^{-2}$ (see Appendix A, § A.1). Consideration of the sizes of the additional terms shows that the criterion for their smallness is that

$$P \gg \max(z^{-1/2}, \kappa^{-2}z^{-3/2}). \quad (\text{B } 3)$$

By definition, in the intermediate region, $z \gg \max(1, \kappa^{-4/3})$, so that the right-hand side of (B 3) is asymptotically small. The assumption that P is large may therefore be relaxed considerably before the skewed approximation loses its validity in the intermediate region.

B.2. The influence of geometry on the skewed approximation

If the assumption that $\epsilon \ll 1$ is relaxed, the explicit expression (2.11) for $f_n(r; s)$ in the wall layer must be replaced by

$$f_n(r; s) = A_{n1}(s)I_0(\lambda^{-1/2}s^{1/2}r) + A_{n2}(s)K_0(\lambda^{-1/2}s^{1/2}r), \quad (\text{B } 4)$$

where I_0 and K_0 are modified Bessel functions; the functions A_{n1} and A_{n2} may be chosen to make the gradient zero at the outer boundary $r = 1 + \epsilon$. In the intermediate region, by assumption $\kappa z/v \ll 1$. Provided $\epsilon \lesssim 1$, this implies that the arguments of the modified Bessel functions in (B 4) are large, and they may be expanded accordingly. (If $\epsilon \gg 1$, that is if the thickness of the wall layer is much larger than the radius of the pipe containing the fluid, we must impose the stronger condition $\lambda^{1/2}\kappa z \ll 1$ to justify this expansion.) Using Abramowitz & Stegun (1972, equations 9.7.1–4), and retaining the leading effect of the curvature of the wall layer, we find that the

boundary condition (2.12) is replaced in the intermediate region by

$$\frac{\partial f_n}{\partial r} = -\kappa s^{1/2} \left(1 + \frac{1}{2}\lambda^{1/2}s^{-1/2} + \dots\right) f_n \quad \text{at } r = 1^-. \quad (\text{B } 5)$$

As just discussed, $\lambda^{1/2}s^{-1/2}$ is small, so that this represents a small perturbation to the exponent in (2.16).

Physically, the skewed approximation is insensitive to the thickness of the wall layer because in the intermediate region tracer has penetrated only a small distance beyond the interface. In addition, in this regime the tracer concentration within the fluid phase is radially uniform. It may therefore be argued that the validity of the skewed approximation (3.1) is not sensitive to the geometrical details of the system, and may be expected to apply also to pipes of non-circular cross-section. In such systems, an effective value of κ must be defined, proportional to the amount of interfacial surface area per unit volume of fluid. In this way the skewed approximation may be expressed, in dimensional terms, as

$$C(\mathbf{R}, Z, T) \sim \frac{\mathcal{M}\mathcal{P}\beta D_w^{1/2}}{2\pi^{1/2}Q^2} \frac{Z}{\Delta T^{3/2}} \exp\left(-\frac{\mathcal{P}^2\beta^2 D_w}{4Q^2} \frac{Z^2}{\Delta T}\right) \quad \text{for } \Delta T > 0, \quad (\text{B } 6)$$

where, in addition to quantities defined in §2, \mathcal{P} is the perimeter of the cross-section of the pipe, and Q is the flow rate.

REFERENCES

- ABRAMOWITZ, M. & STEGUN, I. A. 1972 *Handbook of Mathematical Functions*. Dover.
- ARIS, R. 1959 On the dispersion of a solute by diffusion, convection and exchange between phases. *Proc. R. Soc. Lond. A* **252**, 538–550.
- BALAKOTAIAH, V. & CHANG, H.-C. 1995 Dispersion of chemical solutes in chromatographs and reactors. *Phil. Trans. R. Soc. Lond. A* **351**, 39–75.
- BRENNER, H. & ADLER, P. M. 1982 Dispersion resulting from flow through spatially periodic porous media. II. Surface and intraparticle transport. *Phil. Trans. R. Soc. Lond. A* **307**, 149–200.
- CHATWIN, P. C. 1973 A calculation illustrating effects of the viscous sub-layer on longitudinal dispersion. *Q. J. Mech. Appl. Maths* **26**, 427–439.
- DAVIDSON, M. R. & SCHROTER, R. C. 1983 A theoretical model of absorption of gases by the bronchial wall. *J. Fluid Mech.* **129**, 313–335.
- GILL, W. N. & SANKARASUBRAMANIAN, R. 1970 Exact analysis of unsteady convective flow. *Proc. R. Soc. Lond. A* **316**, 341–350.
- GOLAY, M. J. E. 1958 Theory of Chromatography in open and coated tubular columns with round and rectangular cross-sections. In *Gas Chromatography* (ed. D. H. Desty), p. 36. Butterworths.
- GRADSHTEYN, I. S. & RYZHIK, I. M. 1980 *Table of Integrals, Series and Products*, 2nd edn. Academic.
- LENHOFF, A. M. & LIGHTFOOT, E. N. 1984 The effects of axial diffusion and permeability barriers on the transient response of tissue cylinders. II. Solution in time domain. *J. Theor. Biol.* **106**, 207–238.
- PHILLIPS, C. G. & KAYE, S. R. 1996 A uniformly asymptotic approximation for the development of shear dispersion. *J. Fluid Mech.* **329**, 413–443.
- PHILLIPS, C. G. & KAYE, S. R. 1997 The initial transient of concentration during the development of Taylor dispersion. *Proc. R. Soc. Lond. A* **453**, 2669–2688.
- PHILLIPS, C. G., KAYE, S. R. & ROBINSON, C. D. 1995 Time-dependent transport by convection and diffusion with exchange between two phases. *J. Fluid Mech.* **297**, 373–401.
- PURNAMA, A. 1988 The effect of dead zones on longitudinal dispersion in streams. *J. Fluid Mech.* **186**, 351–377.
- REIS, J. F. G., LIGHTFOOT, E. N., NOBLE, P. T. & CHIANG, A. S. 1979 Chromatography in a Bed of Spheres. *Sep. Sci. Technol.* **14**, 367–394.
- SHANKAR, A. & LENHOFF, A. M. 1991 Dispersion and partitioning in short coated tubes. *Ind. Engng Chem. Res.* **30**, 828–835.

- TAYLOR, G. I. 1953 Dispersion of soluble matter in solvent flowing slowly through a tube. *Proc. R. Soc. Lond. A* **219**, 186–203.
- WESTHAVER, J. W. 1942 Theory of open-tube distillation columns. *Ind. Engng Chem.* **34**, 126–130.
- WESTHAVER, J. W. 1947 Concentration of potassium³⁹ by countercurrent electromigration: some theoretical aspects of the operation. *J. Res. Natl Bur. Stand.* **38**, 169–183.
- YOUNG, W. R. 1988 Arrested shear dispersion and other models of anomalous diffusion. *J. Fluid Mech.* **193**, 129–149.